Acoustic Response Analysis of Medical Percussion using Wavelet Transform and Neural Networks

1st Pilar Zhang Qiu
Dyson School of Design Engineering
Imperial College London
London, United Kingdom
p.zhangqiu@gmail.com

2nd Oliver Thompson
Dyson School of Design Engineering
Imperial College London
London, United Kingdom
olithompson@protonmail.com

3rd Yongxuan Tan
Dyson School of Design Engineering
Imperial College London
London, United Kingdom
jacobtan16@hotmail.com

4th Bennet Cobley
Dyson School of Design Engineering
Imperial College London
London, United Kingdom
ben.cobley@gmail.com

***Abstract*—Medical percussion is a diagnostic procedure used to detect tissue anomalies by acoustic response. Although it is a common in medical practice, there is a limited understanding of its dynamics. This paper examines the acoustic response of percussion and explores how computational techniques may be used to predict the presence and location of tissue anomalies and develop remote assessment devices. In the experiment, audio signals were obtained using a mechanically actuated device percussing a silicone phantom with an embedded nodule at varying depths. The waveforms were analysed using 1-D wavelet transform and classified through a convolutional neural network (CNN). Results showed that a nodule presence closer to the surface of the phantom increases the damping factor and attenuates frequencies between 50 Hz - 400 Hz.**

***Index Terms*—medical percussion, signal analysis, 1D continuous wavelet transform, convolutional neural network (CNN), medical robot, remote healthcare**

I. Introduction

Medical percussion is a preliminary diagnostic procedure whereby the chest, back and abdomen are tapped to determine the conditions of underlying tissues by listening to the acoustic response [1], [2].

The acoustic response elicited by tapping on a body region depends on the ease with which the body wall vibrates and is influenced by underlying organs, strength of the stroke and state of the body wall [3]. These combined form percussion notes. Three key percussion notes are resonance, tympany and dullness; which differ by amplitude, length and frequency [4].

Certain pathologies produce abnormal sounds that are picked up by clinicians during percussion.

Although percussion is a widely accepted practice in medical examination, the literature shows that lack of knowledge and standardisation in percussion can lead to misdiagnosis [5] and disagreements between clinicians on a patient's results [6].

This paper aims to bring automated percussion devices and complex data analysis to Mansy's research [7], in which the acoustic response from condenser microphone-captured abdominal percussions were analysed. More specifically, this paper explores the differences in acoustic waveforms between tissue anomalies using wavelet transform and CNNs of signals captured from a contact microphone.

II. Methods

An acrylic nodule of 11 mm diameter was buried in a platinum-catalyzed silicone Ecoflex 00-10 (Smooth-On, Inc, USA) phantom, with dimensions of 150 mm by 100 mm by 28 mm [8]. The nodule was placed at 2 mm below the surface of the phantom and the phantom could be placed either way up, giving nodule depths of 2 mm and 15 mm (Fig. 1 (b)).

A TIMESETL piezo-electric contact microphone was attached to the surface of the silicone phantom and a previously-developed robotic percussion device [9] was programmed to continuously percuss onto the phantom. The microphone was positioned as close to the impact point as possible, ensuring no clipping of the audio signal occurred (shown in Fig. 1 (a)).

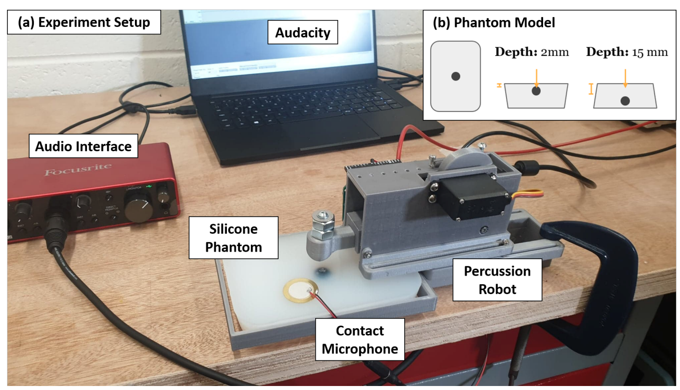

Fig. 1. (a) Robotic percussion device experimental setup. (b) Visual representation of the silicone phantom

The percussion device was programmed to generate datapoints (taps) at a rate of 1.09 Hz over 558 s for each silicone sample side. Audio signals were transmitted through a Focusrite Scarlett 4i4 3rd Gen USB Audio Interface, and recorded with Audacity at 44100 Hz, informed by Nyquist's theorem. The frequency range of interest is the human hearing range, 20 Hz to 20000 Hz.

A. Signal Analysis Using Wavelet Transform

The raw signal was trimmed to individual percussion events through a MATLAB script which identifies local amplitude maximas with an specific amplification-dependent prominence and a minimum distance between peaks of 900ms. The signal was then trimmed 100ms before such points, retrieving a total of 1688 percussion events.

Savitzky-Golay filtering was employed to de-noise the signal whilst preserving maximum concurrence to the original waveform. The de-noised signal was analysed through a 1D Continuous Wavelet Transformations (CWT) coefficient scalogram. This was preferred over Fourier transformations as the time domain contained crucial information on time-localized spectral signal characteristics. The chosen mother wavelet family was Symlet (Sym), widely used in audio analysis and signal damping [10]–[12].

Fig. 2 shows a comparison of scalograms for the average across all samples of close nodule and far nodule signals. The coefficients C represent how closely correlated the wavelet is with specific sections of the signal as well as the signal intensity. These graphs show the effect of damping on the frequency intensities of close nodules.

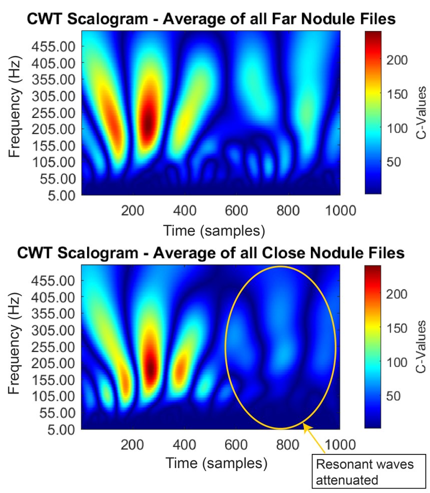

Fig. 2. Graphs for the average coefficient scalograms across all far nodule (top) and close nodule (bottom) percussion samples. Graphs fitted to regions of interest (5-500 Hz).

B. Analysis with a Convolutional Neural Network (CNN)

A CNN was used to verify that the changes in the time and frequency domain observed from the wavelet transform could be used to classify the presence of a nodule. This approach validates our findings over the entire data-set, ensuring that the observed differences are recurrent and reliable and provides the ground work for automatic acoustic response classification in future work.

Greyscale scalograms were generated using Matlab for each of the 1688 taps measured in the experiment. The CNN was trained on 75% of this data, with the renaining scalograms used for validation. The CNN architecture consisted of 3 2D convolutional layers, 2 max pooling layers a flatten layer and a linear layer. Training was stopped when the CNN was able classify the test scalograms with an accuracy of 100%.

Saliency maps were generated for various scalograms which highlight the pixels used by the CNN to inform the successful classification. Fig. 3 shows the salient pixels are in the range of 50 Hz - 200 Hz for both nodules and between 0 s - 0.02s for the close nodule and 0 s - 0.035s for the far nodule. This shows that the lower frequencies are damped by the presence of the nodule, suggesting that both time and frequency domain analysis play an important role in classification. These findings concur with insights from the wavelet transform analysis.

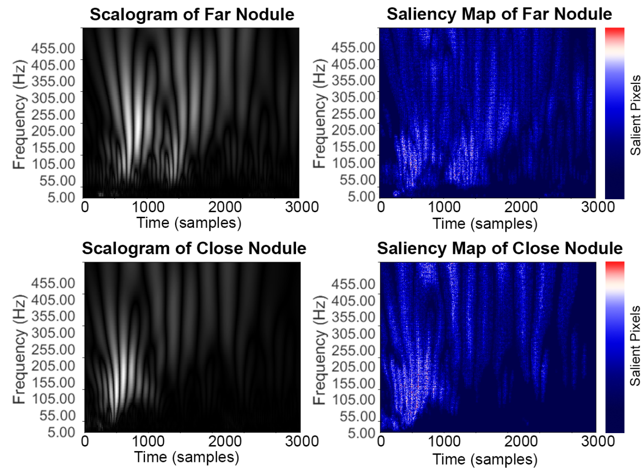

Fig. 3. Greyscale scalogram for the far nodule (top left) and close nodule (bottom left) are shown in comparison with saliency maps (top right and bottom right) from the final layer of the CNN for a single percussion datapoint. Saliency maps show which areas of the input image triggered the CNN's neurons and the salient pixels show which time variant frequency amplitudes are used to classify the presence of a nodule. The important pixel values are outlined in red, with most of the relevant frequencies in the 50 Hz - 200 Hz range over 0.035s

III. Conclusion and Future work

A robotic device was developed to replicate manual percussion and was tested on a silicone phantom containing a hard nodule to simulate a tissue anomaly. Wavelet transform analysis reported clear attenuation of frequency intensities between the percussion of a close (2 mm depth) and a far (15 mm depth) nodule (Fig. 4 - Region B). Saliency maps from the CNN confirmed that the time-localised differences observed in Region A (Fig. 4) can be used to classify the presence of a nodule accurately.

The proposed method, for the first time, provides guidelines to automate percussion examination through audio analysis. Future studies will explore the results in a more representative abdomen model or human participants.

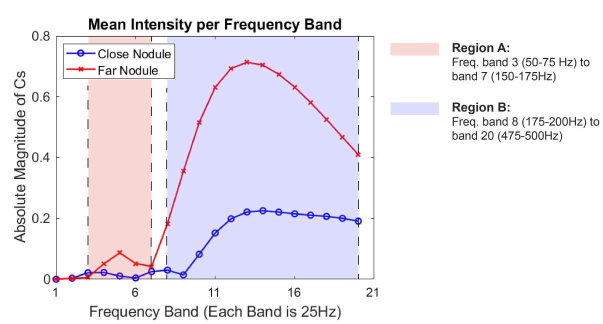

Fig. 4. Intensity difference between samples at specific frequency bands. Each frequency band represents 25 Hz. Region A was shown by the CNN to be a decisive classification factor whereas Region B proves the attenuation of resonant waves in close nodule samples.

REFERENCES

[1] J. B. P. Barth and H. Roger, *Traité pratique d'auscultation; suivi d'un précis de percussion*. Labé, 1860.

[2] D. C. Hall, M. K. Goldstein, and G. H. Stein, "Progress in manual breast examination," *Cancer*, vol. 40, no. 1, pp. 364–370, 1977.

[3] S. E. D. JoVE. (2020) Physical examinations ii. abdominal exam ii: Percussion. [Online]. Available: https://www.jove.com/science-education/10090/abdominal-exam-ii-percussion

[4] J. C. Yernault and A. Bohadana, "Chest percussion," *European Respiratory Journal*, vol. 8, no. 10, pp. 1756–1760, 1995.

[5] J. E. Meidl, Erik J. (1993) Evaluation of liver size by physical examination.

[6] R. Joshi, A. Singh, N. Jajoo, M. Pai, and S. Kalantri, "Accuracy and reliability of palpation and percussion for detecting hepatomegaly: a rural hospital-based study," *Indian Journal of Gastroenterology*, vol. 23, pp. 171–174, 2004.

[7] H. Mansy, T. Royston, and R. Sandler, "Use of abdominal percussion for pneumoperitoneum detection," *Medical and Biological Engineering and Computing*, vol. 40, no. 4, pp. 439–446, 2002.

[8] N. Herzig, L. He, P. Maiolino, S.-A. Abad, and T. Nanayakkara, "Conditioned haptic perception for 3d localization of nodules in soft tissue palpation with a variable stiffness probe," *Plos one*, vol. 15, no. 8, p. e0237379, 2020.

[9] Y. Tan, P. Zhang, O. Thompson, and B. Cobley, "Design and implementation of a robotic device for medical percussion." Imperial College London, 9 2020, unpublished.

[10] D. Yan, L. Xiang, Z. Wang, and R. Wang, "Detection of hmm synthesized speech by wavelet logarithmic spectrum," *Automatic Control and Computer Sciences*, vol. 53, no. 1, pp. 72–79, 2019.

[11] A. Naït-Ali, O. Adam, and J. Motsch, "Modelling and recognition of brainstem auditory evoked potentials using symlet wavelet," *ITBM-RBM*, vol. 21, no. 3, pp. 150–157, 2000.

[12] M. Misiti, Y. Misiti, G. Oppenheim, J.-M. Poggi *et al.*, "Wavelet toolbox user's guide," *The Math Works Inc*, 1996.